Science of the Total Environment 659 (2019) 410–418

Contents lists available at ScienceDirect

Science of the Total Environment

journal homepage: www.elsevier.com/locate/scitotenv

Mapping daily $PM_{2.5}$ at 500 m resolution over Beijing with improved hazy day performance

Yuanyu Xie [a], Yuxuan Wang [a,b,*], Muhammad Bilal [c,**], Wenhao Dong [a]

[a] Ministry of Education Key Laboratory for Earth System Modeling, Department of Earth System Science, Joint Center for Global Change Studies (JCGCS), Tsinghua University, Beijing 100084, China
[b] Department of Earth and Atmospheric Sciences, University of Houston, Houston, TX, USA
[c] School of Marine Sciences, Nanjing University of Information Science & Technology, Nanjing 210044, China

HIGHLIGHTS

- Cloud screen method developed for SARA 500 m AOD improves hazy day performance.
- Daily $PM_{2.5}$ estimated with linear mixed effects model has a CV R^2 of 0.82.
- Population-weighted mean $PM_{2.5}$ varies from 70 to 90 μg m^{-3} by districts in Beijing.
- Distinct pollution patterns identified and exposure estimated for severe hazy days.

GRAPHICAL ABSTRACT

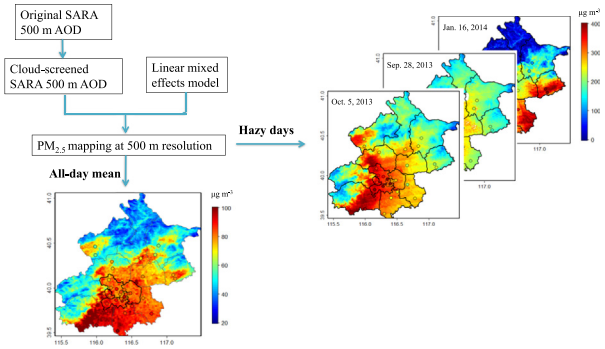

ARTICLE INFO

Article history:
Received 8 November 2018
Received in revised form 24 December 2018
Accepted 24 December 2018
Available online 27 December 2018

Editor: Jianmin Chen

Keywords:
Aerosol optical depth
SARA
$PM_{2.5}$
Sub-km resolution
Hazy day

ABSTRACT

The application of satellite-derived aerosol optical depth (AOD) to infer surface $PM_{2.5}$ has significantly increased the spatial coverage and resolutions (1–10 km) of ground-level $PM_{2.5}$ mapping as required for accurate exposure estimation. The remaining challenge is to further increase the mapping resolution to the sub-km level with improved algorithms to minimize misrepresentation of severe haze as clouds. In this study, we provide the first daily $PM_{2.5}$ estimation over Beijing at a 500 m resolution using AOD from the Simplified Aerosol Retrieval Algorithm (SARA) and linear mixed effects model. A novel cloud screen method is developed which significantly improves data availability during hazy days. The cross-validation R^2 for $PM_{2.5}$ estimations is 0.82 with the cloud-screened SARA AOD. Based on the satellite-predicted high-resolution $PM_{2.5}$ map, all-day population-weighted $PM_{2.5}$ is estimated to be 81.4 μg m^{-3} over Beijing (2.3 times higher than China's NAAQS of 35 μg m^{-3}). Compared to the standard MODIS Dark Target 3 km product which presents a significant percentage of missing data, the 500 m resolution $PM_{2.5}$ mapping derived from SARA AOD reveals distinct pollution patterns and population exposure conditions during severe hazy days, thereby providing valuable information for pollution control and epidemiological studies.

1. Introduction

$PM_{2.5}$ (particulate matter with aerodynamic diameters of <2.5 μm) is ranked as the topmost threat to human health due to its adverse impact on cardiovascular and respiratory system (Lelieveld et al., 2015). Rapid economic development has led to significant increase in precursor

* Correspondence to: Y. Wang, Ministry of Education Key Laboratory for Earth System Modeling, Department of Earth System Science, Joint Center for Global Change Studies (JCGCS), Tsinghua University, Beijing 100084, China.
** Corresponding author.
E-mail addresses: ywang246@central.uh.edu (Y. Wang), muhammad.bilal@connect.polyu.hk (M. Bilal).

https://doi.org/10.1016/j.scitotenv.2018.12.365
0048-9697/

emissions and thus $PM_{2.5}$ concentrations over China (Yuan et al., 2012; Zhang et al., 2012), which results in an adverse effect on population health (Brauer et al., 2016). High PM levels and persistent haze episodes have become one of the most severe environmental concerns in China and attracted great public attention (Xu et al., 2013; Zhang and Cao, 2015). For example, $PM_{2.5}$ levels over the densely populated Beijing are more than double China's National Ambient Air Quality Standard (NAAQS) (Wang et al., 2014; Xie et al., 2015), with episodic extreme concentrations exceeding 500 μg m^{-3}.

Exposure estimation and pollution control require a comprehensive understanding of surface $PM_{2.5}$ concentration distributions at high spatial and temporal resolutions. While in-situ measurements provide the most accurate ground-level $PM_{2.5}$ concentrations, their sparse and uneven distribution results in under-sampling which hinder their ability to fully represent population exposure (van Donkelaar et al., 2010; Xie et al., 2015; Di et al., 2016). Satellite retrieved aerosol optical depth (AOD), an optical indicator of columnar aerosols loading, has been widely adopted to infer surface $PM_{2.5}$ concentrations with more complete spatial coverage (Chu et al., 2003; Liu et al., 2004; van Donkelaar et al., 2010). The accuracy of $PM_{2.5}$ estimations with satellite AOD has been greatly improved by increasing spatial resolutions of AOD products (Chudnovsky et al., 2013a; Chudnovsky et al., 2013b; Xie et al., 2015; Just et al., 2015; Lin et al., 2016) and more realistic representation of the AOD-$PM_{2.5}$ relationships, e.g., by adopting them from advanced statistical models (i.e., linear mixed effects, geographically weighted) or chemical transport models (Liu et al., 2009; van Donkelaar et al., 2013; Ma et al., 2014; Li et al., 2017). Model cross-validation R^2 ranges from 0.6 to 0.9 by taking into consideration of spatially and temporally varying AOD-$PM_{2.5}$ relationships as well as other influencing predicting parameters with higher resolution AOD (Kloog et al., 2011; Chudnovsky et al., 2012; Xie et al., 2015; Lv et al., 2016; Ma et al., 2016b; Zheng et al., 2016).

One crucial limitation of $PM_{2.5}$ estimations using satellite AOD is misrepresentation of severe haze as cloud during the standard cloud mask procedure or subsequent brightness screening (Engel-Cox et al., 2004; Ma et al., 2016a). Several studies have developed cloud screen algorithms to distinguish between cloud and haze and reconstructed information for cloud-contaminated regions (Emili et al., 2011; Li et al., 2013; Cheng et al., 2014; Shang et al., 2014; Shen et al., 2014; Mei et al., 2017b; Shang et al., 2017). Those algorithms are mostly based on the radiative properties of clouds obtained from remote-sensing or ground observations. In this study, we provide daily $PM_{2.5}$ estimations at 500 m resolution over Beijing based on high-resolution AOD. A novel and simplified cloud screen method is developed considering the fact that clouds appear much brighter and present distinct geometric texture compared to the haze layer. High-resolution surface $PM_{2.5}$ mapping is derived using the cloud-screened AOD and the linear mixed effects model. Comparisons with surface monitors and spatial distribution of pollution during severe haze day are presented.

2. Data and methods

2.1. Ground-level $PM_{2.5}$ data and AOD products

Hourly $PM_{2.5}$ concentrations were obtained from the Beijing Municipal Environmental Monitoring Center (http://zx.bjmemc.com.cn). $PM_{2.5}$ was measured with Tapered Element Oscillating Microbalance (TEOM) method and quality controlled according to Environmental Protection standard of China (HJ 618-2011; MEPCN). There are 16 districts in Beijing with Haidian, Chaoyang, Shijingshan, Dongcheng, Xicheng, and Fengtai defined as urban and Yanqing, Huairou, Miyun, Changping, Shunyi, Pinggu, Mentougou, Fangshan, Daxing, and Tongzhou as rural (Fig. 1). The city is surrounded by Taihang mountain in the west and Yanshan mountain in the north, while the urban and southeast regions are low plains. The 35 surface monitors established by Beijing Environmental Protection Bureau sites are distributed within the 16 districts,

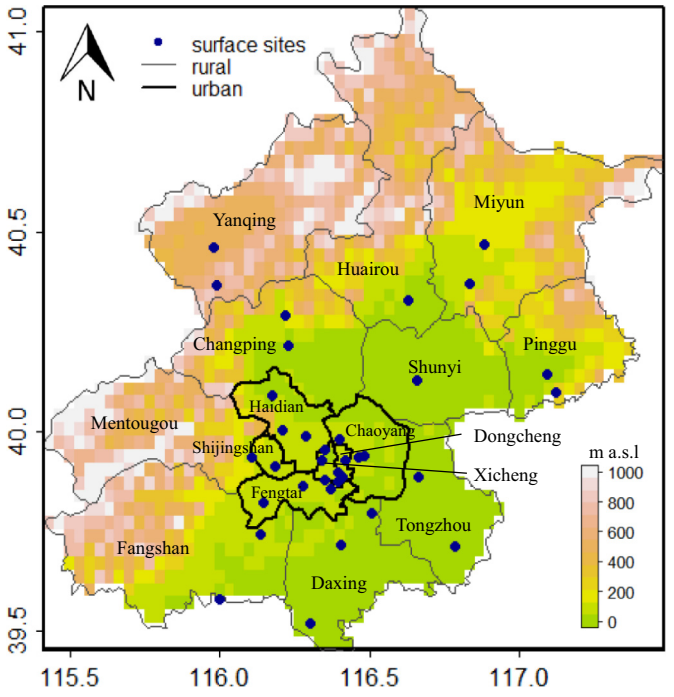

Fig. 1. Topography of Beijing with surface monitors, urban and rural district boundary marked.

with each has one to three sites. Surface $PM_{2.5}$ concentrations measured between 13:00 pm and 14:00 pm local time were averaged to match the Aqua satellite over-passing time. The study period spans from March 2013 to April 2014 with a total length of 394 days when data from surface monitors are available.

The MODerate resolution Imaging Spectroradiometer (MODIS) AOD products have been widely used for surface $PM_{2.5}$ estimations at several spatial resolutions, e.g., 1 km (Multiangle implementation of atmospheric correction, MAIAC), 3 km (Dark Target, DT), and 10 km (DT; Deep Blue, DB). To further increase spatial resolution, Bilal et al. (2013) developed a new Simplified Aerosol Retrieval Algorithm (SARA) to retrieve AOD at 500 m resolution based on MODIS level 1 and level 2 swath products. The SARA requires top–of–atmosphere (TOA) reflectance, surface reflectance, viewing geometry, including solar and sensor angles, and elevation. These parameters are obtained from the MODIS swath products such as the calibrated radiance (MOD02HKM), the geolocation (MOD03), and the surface reflectance products (MOD09) and used together with aerosol properties derived from surface AERONET sites to perform aerosol retrieval. Instead of using the conventional look-up table, the SARA algorithm is based on real viewing geometry and takes into consideration a wide range of aerosol types that better represent complex aerosol mixtures over urban regions. The SARA AOD has been validated over land (Bilal and Nichol, 2015) and water (Bilal et al., 2017a) surfaces. Validation against AERONET AOD over Beijing (Bilal et al., 2014) showed a high correlation ($r > 0.97$) and low bias under both clean and polluted conditions. To ensure better representation of severe haze conditions, the original SARA AOD product is used without undergoing the standard cloud mask process. As SARA algorithm requires AERONET AOD as input data, the total available days for SARA retrieval is 206 days during the study period. The standard 3 km AOD product (MYD04_3K) from Collection 6 is also used in this study for comparison (Munchak et al., 2013).

2.2. Cloud screen method

In this study, we developed a new and simplified screen method to remove clouds under both clean and severe haze conditions. The scheme is based on two assumptions: (1) clouds appear much brighter

and hence their optical depth is greater than that of aerosols; (2) spatial variability of clouds is greater than that of aerosol or haze (Martins, 2002; Emili et al., 2011; Mei et al., 2017b). The cloud screen method is applied to the 206 days of the original product of cloud-contained SARA AOD following the scheme as shown in Fig. 2. We calculated the standard deviation for a 10 km × 10 km box around each grid point. Grids with standard deviation (SD) greater than the mean SD of the entire region is considered as contaminated by clouds. The size of the box is chosen with the consideration of both the spatial scale of clouds and computation efficiency as well. The results showed little difference by slightly changing the box size. Relaxed criteria (half of the mean SD) are applied along the foothill of the city, where topography could lead to greater spatial difference during hazy days.

To further eliminate cloud contamination, we derive a threshold value AOD_t for each day to distinguish between cloud and aerosols at grid level. The threshold AOD_t is calculated as below:

$$AOD_{t,day} = (\alpha + \alpha_{sd}) \times PM_{2.5\ max,day}$$

where α and α_{sd} represent the slope and its standard deviation of linear regression between AOD and surface $PM_{2.5}$ for cloud-free days during the study period. The cloud-free day is defined as days with >80% AOD retrieval in the MODIS 3 km AOD product. The threshold AOD_t is set to the AOD value corresponding to the maximum daily $PM_{2.5}$ values. Grids with values exceeding this threshold value AOD_t would be regarded as cloud and discarded. After two steps of cloud screening, the linear correlation between the cloud-screened SARA 500 m AOD and $PM_{2.5}$ at all sites show a significant improvement compared to the original data (Fig. 2). Average r between SARA AOD and surface $PM_{2.5}$ concentrations increases from 0.62 to 0.72. Most of the high AOD values at the low $PM_{2.5}$ range, representative of cloud conditions, are successfully identified and removed by the cloud-screen method. Detailed statistics for each site also show improved correlations between AOD and $PM_{2.5}$ after cloud screening process (Table S1).

2.3. Model development and validation

The site-collocated AOD is selected from a 500 m grid that contains a surface site. As all surface sites fall in different AOD grids, a total of 35 pairs of AOD-$PM_{2.5}$ are used for model development. Linear mixed effects models were developed to predict surface $PM_{2.5}$ using the cloud-screened SARA 500 m AOD. The mixed effects model to estimate $PM_{2.5}$ using satellite data was proposed first by Lee et al. (2011). The model predicts surface $PM_{2.5}$ concentrations for each site i of the day j ($PM_{2.5,\ ij}$) from collocated satellite AOD (AOD_{ij}) following:

$$PM_{2.5,ij} = (\alpha + u_j) + (\beta + v_j) \times AOD_{ij} + \varepsilon_{ij}$$

$$(u_j v_j) \sim N\left[(00), \sum\right]$$

where α and β represent fixed intercept and slope without temporal variations, u_j and v_j are random intercept and slope at all surface sites, reflecting the changing AOD-$PM_{2.5}$ relationship at daily scale influenced by meteorology, satellite retrieval condition, etc. ε_{ij} is the error term, and $\sum$ is the variance-covariance matrix for the daily varying random effects. Days with less than two pairs of AOD-$PM_{2.5}$ data and negative AOD-$PM_{2.5}$ relationship are excluded during the model fitting process. R^2, mean prediction error (MPE), and root mean square error (RMSE) are three metrics used to evaluate model performance. MPE is estimated as the absolute differences between predicted and measured $PM_{2.5}$ concentrations. RMSE is estimated as the root mean squared differences between predicted and measured $PM_{2.5}$ concentrations.

A 10-fold cross-validation (CV) method is performed on the linear mixed effects models. Specifically, 10% of the data are isolated for model fitting each time and the prediction is performed at those isolated sites using the model derived from all the other sites. The prediction performance is evaluated with observations using R^2, MPE, and RMSE. The CV process assesses the model prediction accuracy on spatial distribution, especially at locations far from the monitoring sites.

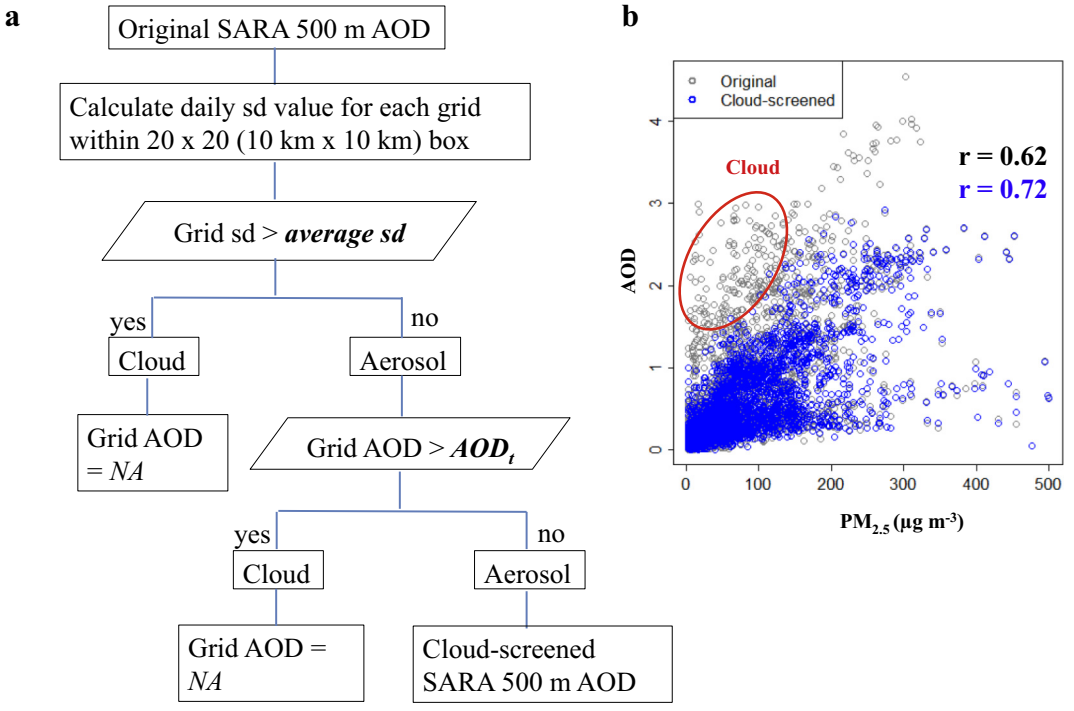

Fig. 2. The cloud screen method (a) and scatter plot (b) of surface $PM_{2.5}$ versus the original SARA 500 m AOD (black) and cloud-screened SARA 500 m AOD (blue). (For interpretation of the references to colour in this figure legend, the reader is referred to the web version of this article.)

3. Results and discussion

3.1. Comparison between SARA 500 m AOD and MODIS 3 km AOD

Fig. 3 compares the original and cloud-screened SARA AOD to that from MODIS 3 km products for the selected days representative of clean (September 21, 2013) and polluted conditions (October 27, 2013). The original SARA AOD at 500 m resolution provides a high-resolution view of aerosols distribution during the clean day (Fig. 3a). However, small clusters of cloud covers are also evident, especially over the southeast region of the city. The cloud screen method applied on SARA 500 m AOD is effective in removing the impacts from clouds while retaining as much as information on aerosols. In comparison, the AOD from MODIS 3 km product has much coarser spatial resolution and contains ~20% of missing data with standard cloud mask process. Linear regression shows a higher correlation coefficient between the surface $PM_{2.5}$ and the cloud-screened SARA AOD ($r = 0.58$), compared to the MODIS 3 km AOD ($r = 0.28$). This indicates that the cloud-screened high-resolution SARA AOD performs better in representing the spatial distribution of surface $PM_{2.5}$. Under haze conditions when dense aerosol layers are typically misidentified as clouds, the cloud-screened SARA AOD is able to retain the pollution information (Fig. 3b). Linear regression between SARA AOD and surface $PM_{2.5}$ show that it captures well the spatial distribution of surface pollution ($r = 0.77$). In comparison, the MODIS 3 km product using the standard cloud mask fails to distinguish between haze and clouds, resulting in missing value almost over the entire region.

Data availability of the cloud-screened SARA 500 m AOD is significantly improved compared to that from the MODIS 3 km AOD during the entire study period. Cloud-screened SARA 500 m AOD has a total number (N) of 4306 available points, significantly higher than those of the 3 km AOD (total N of 2502). Cloud-screened SARA 500 m AOD has about 4 times more data during the cold season (Oct 15th to Apr 14th) as compared to the MODIS 3 km AOD. Data availability for hazy days (>75 μg m^{-3}) is three times for the cloud-screened SARA 500 m AOD compared to the MODIS 3 km AOD. To illustrate the impact of missing AOD on $PM_{2.5}$ estimations, Fig. 4 compares mean $PM_{2.5}$ at the surface sites when averaged over the days with and without satellite AOD during the cold and warm (Apr 15th to Oct 14th) season respectively. The all-data mean $PM_{2.5}$ at the 35 sites ranges from 80.6 (±65.5) μg m^{-3} to 81.3 (±80.4) μg m^{-3} for the warm (cold) season, all exceeding the China's NAAQS annual mean standard of 35 μg m^{-3}. Compared with those 'true' seasonal mean $PM_{2.5}$, average $PM_{2.5}$ during the days with cloud-screened SARA 500 m AOD is comparable during cold season but ~25% lower during the warm season. This suggests that missing AOD tends to occur more frequently in the warm season under relatively more polluted conditions. Since the MODIS 3 km product has more days with missing AOD, the associated under-sampling bias is significantly larger. Relative to the 'true' seasonal mean, average $PM_{2.5}$ during days with MODIS 3 km AOD is 37% and up to ~60% lower during the warm and cold reason. The lower under-sampling bias of SARA 500 m AOD is mainly attributed to the new cloud screen method, which greatly improved AOD retrieval under haze conditions.

Daily time series of $PM_{2.5}$ averaged at all the sites show a good correlation with collocated cloud-screened SARA 500 m AOD ($r = 0.81$, Fig. 4c). The correlations for the cold and warm season are 0.83 and 0.89, respectively. The corresponding correlation r is much smaller for MODIS 3 km AOD, with values of 0.46 and 0.74, respectively. The improved correlation of cloud-screened SARA 500 m AOD compared to MODIS 3 km AOD can be partly attributed to better representation of haze conditions. The above comparisons indicate that the cloud-screened SARA AOD product significantly improves upon the standard 3 km product in terms of (1) data availability, (2) spatial resolution, and (3) ability in detecting haze.

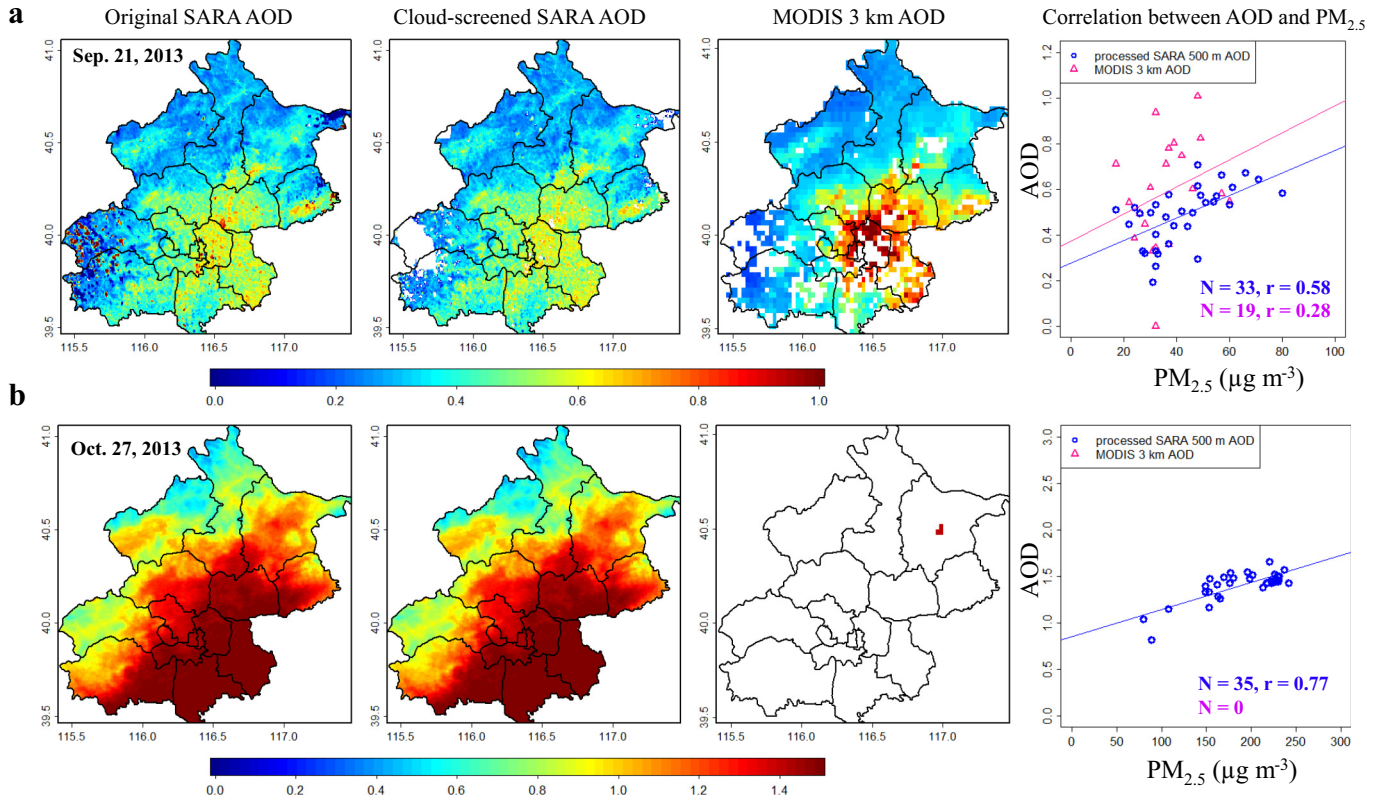

Fig. 3. Illustration of the effects of the cloud screen process applied on original SARA 500 m AOD under clean (a) and polluted (b) conditions. Together shown are correlations between $PM_{2.5}$ and AOD on the same day.

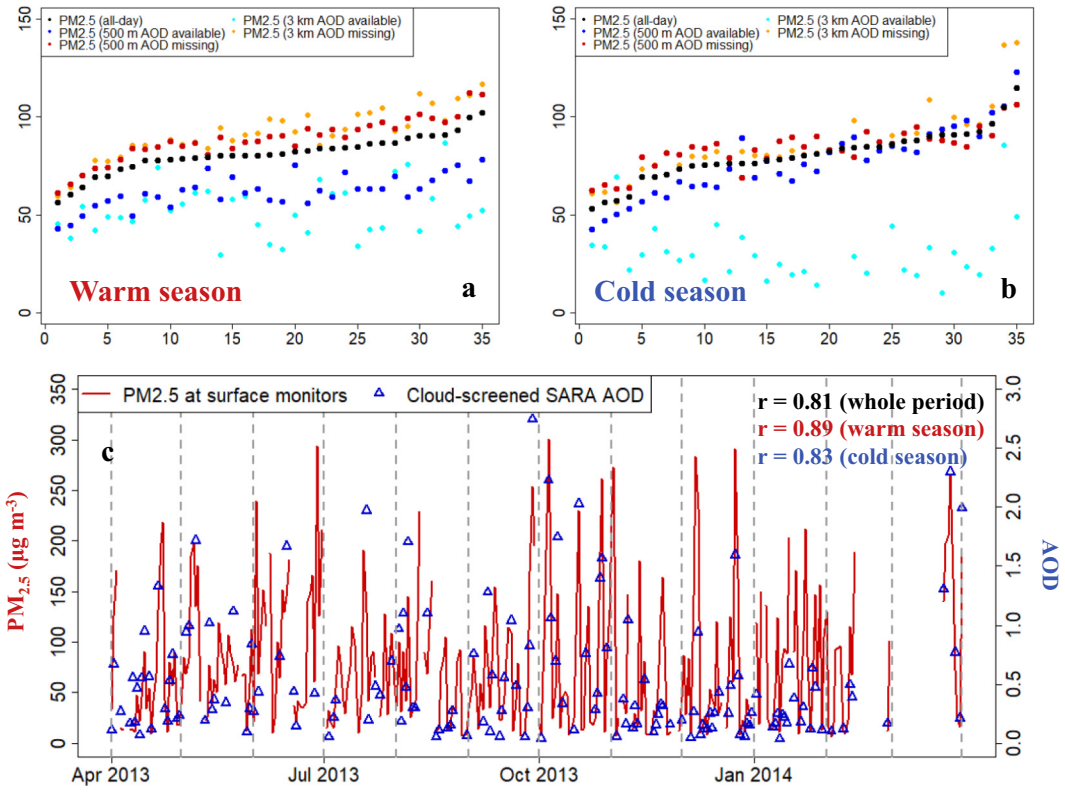

Fig. 4. $PM_{2.5}$ concentrations averaged during the entire study period (black), at available/missing SARA 500 m AOD (blue/red) and MODIS 3 km AOD (cyan/orange) for each site during the warm (a) and cold (b) season, the sites are shown in ascending order of the site-specific annual mean $PM_{2.5}$ concentration; daily time series of site-averaged $PM_{2.5}$ and site-collocated cloud-screened SARA 500 m AOD (c). (For interpretation of the references to colour in this figure legend, the reader is referred to the web version of this article.)

3.2. Mixed-effects model fitting and validation

With data screening process, a total of 123 days with 3118 pairs of the cloud-screened AOD-$PM_{2.5}$ are used for model fitting. The performances of the linear mixed effects model are listed in Table 1. The fixed term of the intercept and slope is 5.51 ($p < 0.001$) and 151.05 ($p < 0.001$), with the standard errors being 4.89 and 17.16, respectively. The daily specific intercept and slope have a standard deviation of 38.52 and 138.55, respectively. The large standard deviation indicates significant variations of the AOD-$PM_{2.5}$ relationships on a daily basis. The overall R^2 between the predicted and measured $PM_{2.5}$ is 0.84 from the mixed effects model (Fig. 5). This indicates that the cloud-screened SARA 500 m AOD product can explain on average 84% of the observed daily $PM_{2.5}$ variability. The overall MPE and RMSE are 17.69 μg m^{-3} and 28.63 μg m^{-3}. The mixed effects model has a slightly higher correlation and smaller MPE and RMSE when fitting the model for the warm season than it does for the cold season (Table 1). The mean slope for the warm and cold season are 88.03 (SD = 33.83) and 203.29 (SD = 176.21), respectively. The larger slope and SD for the cold season reflects more concentrated $PM_{2.5}$ layers near the surface and greater day-to-day variations of the AOD-$PM_{2.5}$ relationship (Guo et al., 2017; Zheng et al., 2017). Less variation is found for the intercept term between the two seasons.

The 10-fold CV results are also shown in Table 1 for linear mixed effects models for the three periods. The R^2 ranges from 0.80 to 0.86 during different periods, being slightly lower than that derived from the linear mixed effects model. The MPE and RMSE range from 15.07 μg m^{-3}–21.97 μg m^{-3} and 24.14 μg m^{-3} to 35.27 μg m^{-3}. Overall, the CV process suggests that the linear mixed effects model performs well in predicting surface $PM_{2.5}$ concentrations during different periods.

Table 1
Model performance statistics for the mixed effects model.

	Input dataset	R^2	MPE (μg m^{-3})	RMSE (μg m^{-3})
Mixed effects model	Whole period	0.84	17.69	28.63
	Warm season	0.87	14.23	22.59
	Cold season	0.83	20.08	31.86
Cross validation	Whole period	0.82	19.57	31.88
	Warm season	0.86	15.07	24.14
	Cold season	0.80	21.97	35.27

3.3. Predicted mean and hazy day surface $PM_{2.5}$

All-day mean ground-level $PM_{2.5}$ concentrations derived from the cloud-screened SARA 500 m AOD are mapped in Fig. 6. Days with <50% of spatial coverage is neglected and the remaining 113 days were averaged. All-day mean $PM_{2.5}$ from surface monitors is 80.8 μg m^{-3}. Satellite predicted $PM_{2.5}$ well captures the mean concentrations and the southeast-northwest gradients at the site locations (r = 0.62). Of the 35 surface monitors, satellite predicted all-day mean $PM_{2.5}$ concentrations at 21 monitors are within 10% of the surface observed values. Satellite-derived annual $PM_{2.5}$ for the entire Beijing is 64.9 μg m^{-3}, ~20% lower than the average of the site measurements. The lower pollution level indicated by satellite is due to an uneven distribution of surface monitor sites, with more sites located over urban and developed suburban regions and fewer sites in the mountainous region. Spatially, there is a strong southeast-to-northwest decreasing gradient throughout the year. Mean $PM_{2.5}$ is 82.4 μg m^{-3} for urban districts and 63.3 μg m^{-3} for rural districts. Such a gradient results from a combination of topography, land use and regional transport. Local emissions are relatively low and the high elevation is unfavorable for pollution transport over the

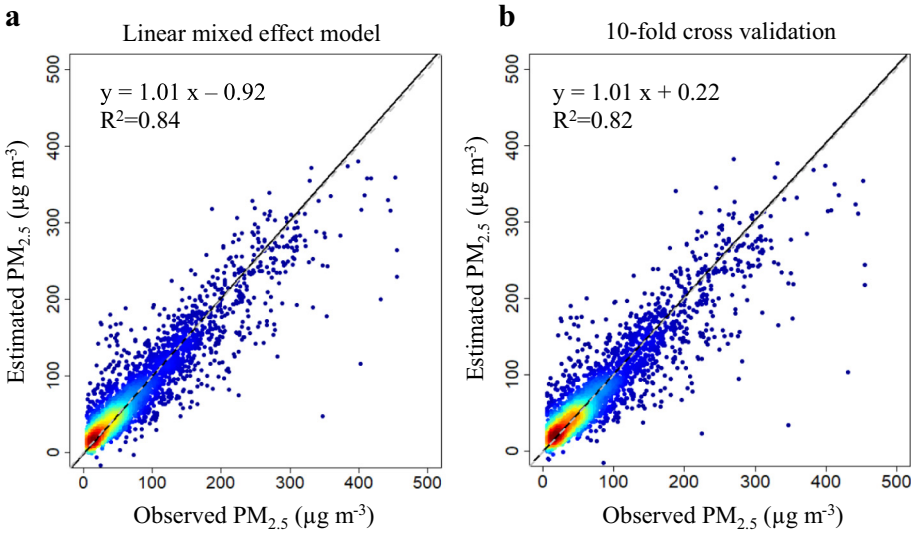

Fig. 5. Scatter plots for linear mixed effects model (a) and the corresponding cross-validation (b) results between measured and estimated $PM_{2.5}$ for the entire study period.

western and northern mountainous regions. The urban and southern regions are more polluted due to higher local emissions and frequent pollution transport from the southern industrialized cities in the North China Plain.

The high-resolution $PM_{2.5}$ maps provide valuable information for population exposure estimation. The total population is 24.68 million in 2010 based on the 1 km population data derived from population census and land use information (Fu et al., 2014). A total of 15.41 million (62.44%) reside in urban districts and the rest in suburban districts. Population density (thousand people per square kilometer) for the urban districts ranges from 7.4 to 52, much larger than that of the rural districts (0.3–1.4). All-day mean population-weighted $PM_{2.5}$ is 81.4 μg m^{-3}, 25% higher than the areal mean as higher population density in the more polluted urban districts. This value is close (within 1%) to average $PM_{2.5}$ concentrations at the 35 sites since most of the monitors are located in the regions with higher population density. This suggests that $PM_{2.5}$ concentration from surface monitors provide a reasonable estimate of population exposure at the city level. Almost the entire city (>97%) and its population (>98%) are exposed to risky $PM_{2.5}$ pollution (>35 μg m^{-3}).

However, there are large differences between the $PM_{2.5}$ derived from the satellite and that from the surface sites at the district level (Fig. 6b). The satellite-derived population-weighted $PM_{2.5}$ is lower than mean $PM_{2.5}$ from surface sites at eight districts, with the largest difference found at Dongcheng district (−11%). For the two most densely populated Dongcheng and Xicheng districts, surface measurements tend to overestimate average pollution condition by up to 10 μg m^{-3} compared to satellite predictions. This overestimation is probably due to site location near traffic or pollution source. Inclusion of satellite predictions thus provides a more accurate evaluation of the overall pollution conditions over these densely populated districts. Meanwhile, higher pollution level is suggested by satellite-derived $PM_{2.5}$ for the other districts. For example, the population-weighted $PM_{2.5}$ is up to 5 μg m^{-3} (6%) higher than that from the surface site at an urban district (Shijingshan) and up to 10 μg m^{-3} (16%) higher at a rural district (Yanqing). This indicates that current surface sites underestimate the pollution levels at these districts due to under-sampling because of the relatively sparse site distribution. Thus, population exposure estimated based solely on the surface sites could underestimate the real health risk over these regions.

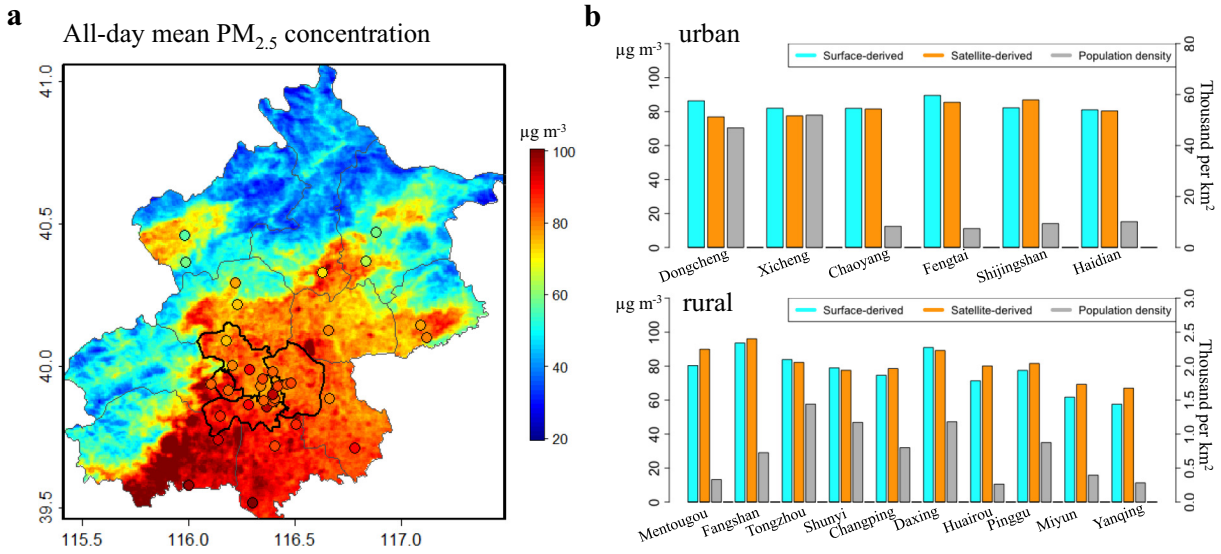

Fig. 6. Satellite-derived all-day mean $PM_{2.5}$ concentration overlapped with that measured at surface monitors (filled circles) (a), and comparison of satellite-derived and surface monitors-measured $PM_{2.5}$ for each district together with population density (b).

As one of the key improvements of SARA AOD on the representation of pollution during hazy days, Fig. 7 presents the spatial distribution of the predicted surface $PM_{2.5}$ concentration during six heavily polluted days. Daily mean $PM_{2.5}$ of all the days selected is >150 μg m^{-3}, with spatial coverage >50%. Compared to the all-day mean pollution condition, distinct pollution patterns can be identified for the polluted days. There is a clear west to east pollution gradient indicated by both surface measurement and satellite estimations on Oct. 5, 2013, when surface mean $PM_{2.5}$ is >300 μg m^{-3}. Such pollution pattern reflects pollution accumulation along the foothill of western mountains under the prevailing southeast wind. We calculated the percentage of the population falling within five categories of pollution levels. During this hazy day, 73% population are exposed to extremely polluted condition ($PM_{2.5}$ > 300 μg m^{-3}) and 26% are under heavily polluted condition ($PM_{2.5}$ between 200 and 300 μg m^{-3}), suggesting a severe health risk for the entire city. Similar pollution and wind pattern are also found on Sep. 28, 2013 as southeast wind favors pollution accumulation in the city. More than 98% of the population is under heavily or extremely polluted conditions during that day.

By comparison, the most polluted regions lie in the southern and eastern part of the city on Jan.16, 2014 and Dec.25, 2013. The center of the city and northwest part are relatively clean, resulting in spatially heterogeneous pollution pattern (large standard deviation). The diverse pollution pattern is attributed to clean air blown from northwest and northeast that has moved away from the pollution in the northern part of the city. As clean air has not wrapped out the pollution over the southern and eastern part, 51% of the population is still under heavily or extremely polluted conditions on Jan.16, 2014 with rest of 48% under slightly polluted conditions. Stronger wind from the northwest alleviates the pollution condition on Dec.25, 2013, resulting in

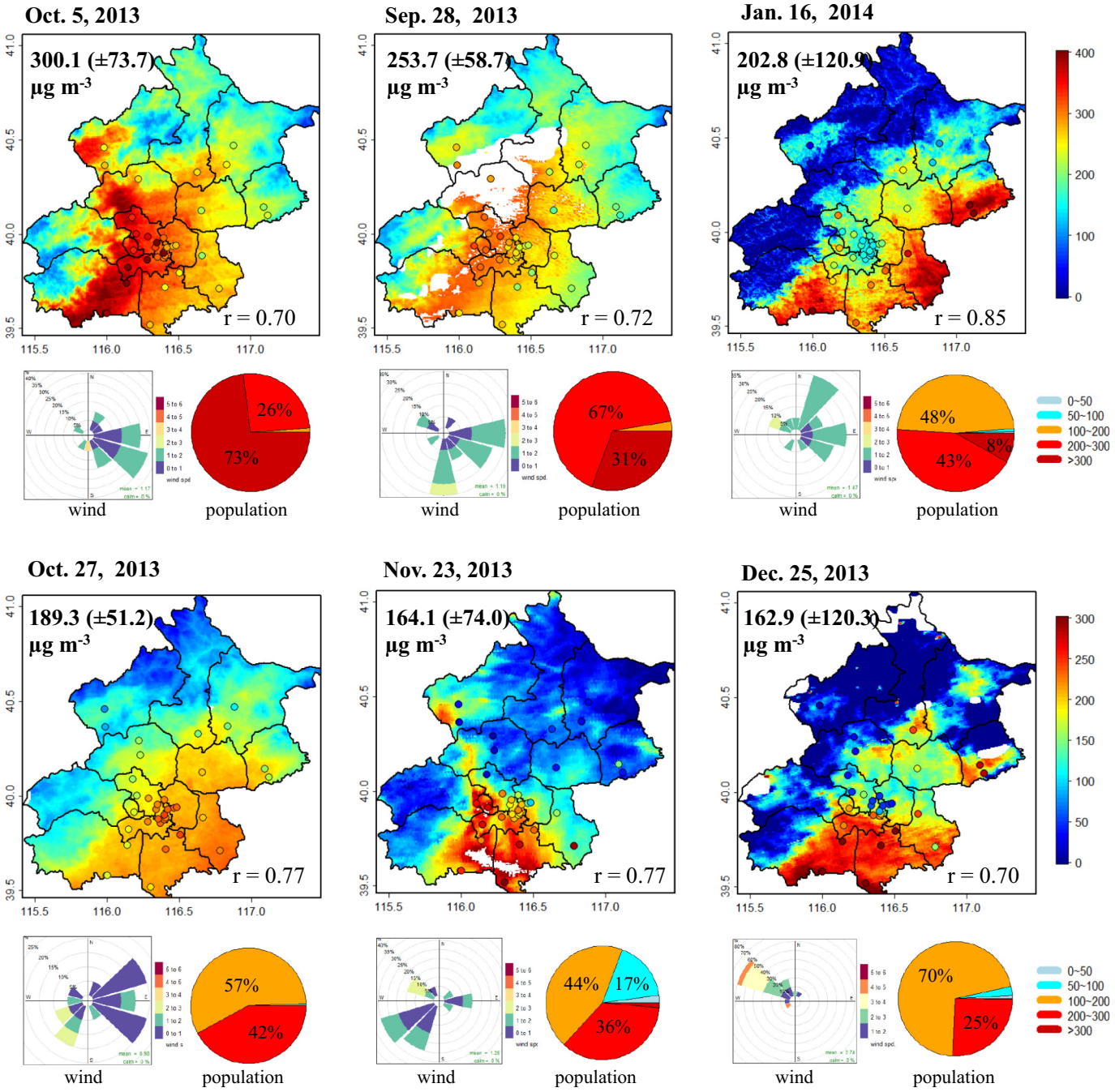

Fig. 7. Satellite-derived $PM_{2.5}$ mapping for severe hazy days and the corresponding wind rose and population exposure estimations.

25% under heavily and 70% under slightly polluted condition. On Oct.27, 2013, mild wind leads to a relatively homogeneous pollution condition all over the city (small standard deviation), with 42% population exposed to heavily polluted condition and 57% under slightly polluted condition. The pollution distribution for Nov.23, 2013 reflects a typical south-to-north transport pattern. Southwest wind results in significant pollutant transport from Heibei Province with dense industry. While 17% of the population is still having relatively clean air, 80% of the population is already affected by the pollution transported from the south. The high-resolution pollution map on daily scale provides valuable information on the spatial distribution of pollution and population exposure during heavily polluted days. In comparison, the MODIS 3 km product has a significant percentage of missing data (Fig. S1), hindering its representation for hazy days.

4. Discussion and conclusion

The 500 m resolution $PM_{2.5}$ mapping over Beijing in this paper has several improvements compared to our previous estimations using the 3 km MODIS AOD (Xie et al., 2015). First, the data availability has greatly increased during the cold season. The new cloud screen method developed here allows a better separation of haze from clouds in satellite AOD, resulting in a large increase in data availability for heavily polluted regions like Beijing. Second, there is a six-fold increase (from 3 km to 500 m) in the spatial resolution of the predicted surface $PM_{2.5}$ distribution. The spatial and temporal heterogeneity of $PM_{2.5}$ is revealed more clearly at the 500 m resolution. As a result of those two improvements, long-term population-weighted mean $PM_{2.5}$ estimated in this study is 81.4 μg m^{-3}, which is 59% higher than our previous estimation of 51.2 μg m^{-3}. Third, the model prediction ($R^2 = 0.84$) and cross-validation ($R^2 = 0.82$) performance is better than that using the 3 km AOD (prediction $R^2 = 0.81$–0.83, and CV $R^2 = 0.75$–0.79).

This is the first implementation of the 500 m SARA AOD for $PM_{2.5}$ estimations over Beijing; the other two studies using SARA 500 m AOD focused on Hong Kong and eastern China respectively (Bai et al., 2016; Bilal et al., 2017b). Our results show a higher prediction accuracy (prediction $R^2 = 0.84$) compared to R^2 of 0.61 in Bilal et al. (2017b). Bai et al. (2016) showed a higher CV R^2 of 0.87 using geographically and temporally weighted regression. Their study period is only three months as compared to one year in this study, and their model relies on multiple input parameters while the model in this study uses AOD as the single input. Other studies provided $PM_{2.5}$ estimations based on satellite AOD over China with a spatial resolution ranging from 1 to 12 km, coarser than that presented in this study (Ma et al., 2014; Li et al., 2015; Fang et al., 2016; Lv et al., 2016; Ma et al., 2016b; Zou et al., 2016; You et al., 2016; Zang et al., 2017; Lv et al., 2017). The CV R^2 reported from these previous studies over China range from 0.58 to 0.80, and our result is at the high end. Besides, the model accuracy achieved in this study are comparable to studies over the less polluted United States with the prediction or CV R^2 in the range of 0.84 to 0.92 (Chudnovsky et al., 2012; Kloog et al., 2014; Di et al., 2016).

Although our cloud screen method shows a good performance in distinguishing between cloud and haze, the underlying assumptions may not always hold true. For example, the method is not applicable to cases when thin clouds coexist with thick aerosol layers (Calbó et al., 2017; Mei et al., 2017a). While an aerosol layer generally appears smoother than clouds, fires or intense emissions may result in higher spatial variability, which would be removed during the cloud screen process. Residue cloud may exist as there may not be a clear border between cloud and aerosol (Koren et al., 2007; Sogacheva et al., 2017). Furthermore, uncertainties also exist in satellite retrievals, surface measurement and the linear assumption of the mixed effects model (Guo et al., 2017). In spite of these uncertainties, the present study is the first attempt of using satellite AOD to derive surface $PM_{2.5}$ at a 500 m resolution for Beijing with better model prediction and cross-validation performance compared to previously published studies, which were mostly at spatial resolutions coarser than 1 km. The high-resolution daily surface $PM_{2.5}$ map will provide valuable data to support pollution monitoring and prediction, exposure estimation, and air pollution advisory for the public.

Acknowledgment

We gratefully acknowledge the Beijing Municipal Environmental Monitoring Center in proving the hourly $PM_{2.5}$ data through http://zx.bjmemc.com.cn. The MODIS 3 km AOD product can be accessed through https://ladsweb.modaps.eosdis.nasa.gov/. The SARA 500 m AOD product, the cloud screened SARA AOD and $PM_{2.5}$ estimation data is available upon request to the corresponding author. This research was supported by the National Key Basic Research Program of China (2014CB441302), National Science Foundation of China (41374013) and the Startup Foundation for Introduction Talent of NUIST (2017r107). We thank Dr. Y. Bai's group for preparing the surface $PM_{2.5}$ data. We are also thankful to Devin White (Oak Ridge National Laboratory) for MODIS Conversion Tool Kit (MCTK).

Appendix A. Supplementary data

Supplementary data to this article can be found online at https://doi.org/10.1016/j.scitotenv.2018.12.365.

References

Bai, Y. Wu L., Qin, K., Zhang, Y., Shen, Y., Geographically, Zhou Y.A., 2016. Temporally weighted regression model for ground-level $PM_{2.5}$ estimation from satellite-derived 500 m resolution AOD. Remote Sens. 8 (3), 262.
Bilal, M., Nichol, J.E., 2015. Evaluation of MODIS aerosol retrieval algorithms over the Beijing-Tianjin-Hebei region during low to very high pollution events. J. Geophys. Res. Atmos. 120, 7941–7957.
Bilal, M., Nichol, J.E., Bleiweiss, M.P., Dubois, D., 2013. A Simplified high resolution MODIS Aerosol Retrieval Algorithm (SARA) for use over mixed surfaces. Remote Sens. Environ. 136, 135–145.
Bilal, M., Nichol, J.E., Chan, P.W., 2014. Validation and accuracy assessment of a Simplified Aerosol Retrieval Algorithm (SARA) over Beijing under low and high aerosol loadings and dust storms. Remote Sens. Environ. 153, 50–60.
Bilal, M., Nazeer, M., Nichol, J.E., 2017a. Validation of MODIS and VIIRS derived aerosol optical depth over complex coastal waters. Atmos. Res. 186, 43–50.
Bilal, M., Nichol, J.E., Spak, S.N., 2017b. A new approach for estimation of fine particulate concentrations using satellite aerosol optical depth and binning of meteorological variables. Aerosol Air Qual. Res. 17, 356–367.
Brauer, M., Freedman, G., Frostad, J., van Donkelaar, A., Martin, R.V., Dentener, F., et al., 2016. Ambient air pollution exposure estimation for the global burden of disease 2013. Environ. Sci. Technol. 50, 79–88.
Calbó, J., Long, C.N., González, J.-A., Augustine, J., McComiskey, A., 2017. The thin border between cloud and aerosol: sensitivity of several ground based observation techniques. Atmos. Res. 196, 248–260.
Cheng, Q., Shen, H., Zhang, L., Yuan, Q., Zeng, C., 2014. Cloud removal for remotely sensed images by similar pixel replacement guided with a spatio-temporal MRF model. ISPRS J. Photogramm. Remote Sens. 92, 54–68.
Chu, D.A., Kaufman, Y.J., Zibordi, G., Chern, J.D., Mao, J., Li, C.C., et al., 2003. Global monitoring of air pollution over land from the Earth Observing System-Terra Moderate Resolution Imaging Spectroradiometer (MODIS). J. Geophys. Res.-Atmos. 108.
Chudnovsky, A.A., Lee, H.J., Kostinski, A., Kotlov, T., Koutrakis, P., 2012. Prediction of daily fine particulate matter concentrations using aerosol optical depth retrievals from the Geostationary Operational Environmental Satellite (GOES). J. Air Waste Manage. Assoc. 62, 1022–1031.
Chudnovsky, A., Tang, C., Lyapustin, A., Wang, Y., Schwartz, J., Koutrakis, P., 2013a. A critical assessment of high-resolution aerosol optical depth retrievals for fine particulate matter predictions. Atmos. Chem. Phys. 13, 10907–10917.
Chudnovsky, A.A., Kostinski, A., Lyapustin, A., Koutrakis, P., 2013b. Spatial scales of pollution from variable resolution satellite imaging. Environ. Pollut. 172, 131–138.
Di, Q., Kloog, I., Koutrakis, P., Lyapustin, A., Wang, Y., Schwartz, J., 2016. Assessing $PM_{2.5}$ exposures with high spatiotemporal resolution across the continental United States. Environ. Sci. Technol. 50, 4712–4721.
Emili, E., Lyapustin, A., Wang, Y., Popp, C., Korkin, S., Zebisch, M., et al., 2011. High spatial resolution aerosol retrieval with MAIAC: application to mountain regions. J. Geophys. Res. Atmos. 116.
Engel-Cox, J.A., Holloman, C.H., Coutant, B.W., Hoff, R.M., 2004. Qualitative and quantitative evaluation of MODIS satellite sensor data for regional and urban scale air quality. Atmos. Environ. 38, 2495–2509.
Fang, X., Zou, B., Liu, X., Sternberg, T., Zhai, L., 2016. Satellite-based ground $PM_{2.5}$ estimation using timely structure adaptive modeling. Remote Sens. Environ. 186, 152–163.

Fu, J.Y., Jiang, D., Huang, Y.H., 2014. 1 km Grid Population Dataset of China (PopulationGrid_China). Global Change Research Data Publishing & Repository https://doi.org/10.3974/geodb.2014.01.06.V1 http://www.geodoi.ac.cn/.

Guo, J., Xia, F., Zhang, Y., Liu, H., Li, J., Lou, M., et al., 2017. Impact of diurnal variability and meteorological factors on the $PM_{2.5}$ - AOD relationship: implications for $PM_{2.5}$ remote sensing. Environ. Pollut. 221, 94–104.

Just, A.C., Wright, R.O., Schwartz, J., Coull, B.A., Baccarelli, A.A., Tellez-Rojo, M.M., et al., 2015. Using high-resolution satellite aerosol optical depth to estimate daily $PM_{2.5}$ geographical distribution in Mexico City. Environ. Sci. Technol. 49, 8576–8584.

Kloog, I., Koutrakis, P., Coull, B.A., Lee, H.J., Schwartz, J., 2011. Assessing temporally and spatially resolved $PM_{2.5}$ exposures for epidemiological studies using satellite aerosol optical depth measurements. Atmos. Environ. 45, 6267–6275.

Kloog, I., Chudnovsky, A.A., Just, A.C., Nordio, F., Koutrakis, P., Coull, B.A., et al., 2014. A new hybrid spatio-temporal model for estimating daily multi-year $PM_{2.5}$ concentrations across northeastern USA using high resolution aerosol optical depth data. Atmos. Environ. 95, 581–590.

Koren, I., Remer, L.A., Kaufman, Y.J., Rudich, Y., Martins, J.V., 2007. On the twilight zone between clouds and aerosols. Geophys. Res. Lett. 34.

Lee, H.J., Liu, Y., Coull, B.A., Schwartz, J., Koutrakis, P., 2011. A novel calibration approach of MODIS AOD data to predict $PM_{2.5}$ concentrations. Atmos. Chem. Phys. 11, 7991–8002.

Lelieveld, J., Evans, J.S., Fnais, M., Giannadaki, D., Pozzer, A., 2015. The contribution of outdoor air pollution sources to premature mortality on a global scale. Nature 525, 367–371.

Li, S., Chen, L., Xiong, X., Tao, J., Su, L., Han, D., et al., 2013. Retrieval of the haze optical thickness in North China Plain using MODIS data. IEEE Trans. Geosci. Remote Sens. 51, 2528–2540.

Li, R., Gong, J., Chen, L., Wang, Z., 2015. Estimating ground-level $PM_{2.5}$ using fine-resolution satellite data in the megacity of Beijing, China. Aerosol Air Qual. Res. 15, 1347–1356.

Li, T., Shen, H., Zeng, C., Yuan, Q., Zhang, L., 2017. Point-surface fusion of station measurements and satellite observations for mapping $PM_{2.5}$ distribution in China: methods and assessment. Atmos. Environ. 152, 477–489.

Lin, C., Li, Y., Lau, A.K.H., Deng, X., Tse, T.K.T., Fung, J.C.H., et al., 2016. Estimation of long-term population exposure to $PM_{2.5}$ for dense urban areas using 1-km MODIS data. Remote Sens. Environ. 179, 13–22.

Liu, Y., Park, R.J., Jacob, D.J., Li, Q., Kilaru, V., Sarnat, J.A., 2004. Mapping annual mean ground-level $PM_{2.5}$ concentrations using Multiangle Imaging Spectroradiometer aerosol optical thickness over the contiguous United States. J. Geophys. Res. Atmos. 109.

Liu, Y., Paciorek, C.J., Koutrakis, P., 2009. Estimating regional spatial and temporal variability of $PM_{2.5}$ concentrations using satellite data, meteorology, and land use information. Environ. Health Perspect. 117, 886–892.

Lv, B., Hu, Y., Chang, H.H., Russell, A.G., Bai, Y., 2016. Improving the accuracy of daily $PM_{2.5}$ distributions derived from the fusion of ground-level measurements with aerosol optical depth observations, a case study in North China. Environ. Sci. Technol. 50, 4752–4759.

Lv, B., Hu, Y., Chang, H.H., Russell, A.G., Cai, J., Xu, B., et al., 2017. Daily estimation of ground-level $PM_{2.5}$ concentrations at 4 km resolution over Beijing-Tianjin-Hebei by fusing MODIS AOD and ground observations. Sci. Total Environ. 580, 235–244.

Ma, Z., Hu, X., Huang, L., Bi, J., Liu, Y., 2014. Estimating ground-level $PM_{2.5}$ in China using satellite remote sensing. Environ. Sci. Technol. 48, 7436–7444.

Ma, X., Wang, J., Yu, F., Jia, H., Hu, Y., 2016a. Can MODIS AOD be employed to derive $PM_{2.5}$ in Beijing-Tianjin-Hebei over China? Atmos. Res. 181, 250–256.

Ma, Z., Hu, X., Sayer, A.M., Levy, R., Zhang, Q., Xue, Y., et al., 2016b. Satellite-based spatiotemporal trends in $PM_{2.5}$ concentrations: China, 2004–2013. Environ. Health Perspect. 124, 184–192.

Martins, J.V., 2002. MODIS Cloud screening for remote sensing of aerosols over oceans using spatial variability. Geophys. Res. Lett. 29.

Mei, L., Rozanov, V., Vountas, M., Burrows, J.P., Levy, R.C., Lotz, W., 2017a. Retrieval of aerosol optical properties using MERIS observations: algorithm and some first results. Remote Sens. Environ. 197, 125–140.

Mei, L., Vountas, M., Gómez-Chova, L., Rozanov, V., Jäger, M., Lotz, W., et al., 2017b. A Cloud masking algorithm for the XBAER aerosol retrieval using MERIS data. Remote Sens. Environ. 197, 141–160.

MEPCN, d. Determination of atmospheric articles PM_{10} and $PM_{2.5}$ in ambient air by gravimetric method. Available at:. http://english.mep.gov.cn/standards_reports/, Accessed date: 21 February 2017.

Munchak, L.A., Levy, R.C., Mattoo, S., Remer, L.A., Holben, B.N., Schafer, J.S., et al., 2013. MODIS 3 km aerosol product: applications over land in an urban/suburban region. Atmos. Meas. Tech. 6, 1747–1759.

Shang, H., Chen, L., Tao, J., Su, L., Jia, S., 2014. Synergetic use of MODIS cloud parameters for distinguishing high aerosol loadings from clouds over the North China Plain. IEEE J. Sel. Top. Appl. Earth Obs. Remote Sens. 7, 4879–4886.

Shang, H., Chen, L., Letu, H., Zhao, M., Li, S., Bao, S., 2017. Development of a daytime cloud and haze detection algorithm for Himawari-8 satellite measurements over central and eastern China. J. Geophys. Res. Atmos. 122, 3528–3543.

Shen, H., Li, H., Qian, Y., Zhang, L., Yuan, Q., 2014. An effective thin cloud removal procedure for visible remote sensing images. ISPRS J. Photogramm. Remote Sens. 96, 224–235.

Sogacheva, L., Kolmonen, P., Virtanen, T.H., Rodriguez, E., Saponaro, G., de Leeuw, G., 2017. Post-processing to remove residual clouds from aerosol optical depth retrieved using the Advanced Along Track Scanning Radiometer. Atmos. Meas. Tech. 10, 491–505.

van Donkelaar, A., Martin, R.V., Brauer, M., Kahn, R., Levy, R., Verduzco, C., et al., 2010. Global estimates of ambient fine particulate matter concentrations from satellite-based aerosol optical depth: development and application. Environ. Health Perspect. 118, 847–855.

van Donkelaar, A., Martin, R.V., Spurr, R.J.D., Drury, E., Remer, L.A., Levy, R.C., et al., 2013. Optimal estimation for global ground-level fine particulate matter concentrations. J. Geophys. Res.-Atmos. 118, 5621–5636.

Wang, Y.X., Zhang, Q.Q., Jiang, J.K., Zhou, W., Wang, B.Y., He, K.B., et al., 2014. Enhanced sulfate formation during China's severe winter haze episode in January 2013 missing from current models. J. Geophys. Res.-Atmos. 119, 16.

Xie, Y., Wang, Y., Zhang, K., Dong, W., Lv, B., Bai, Y., 2015. Daily estimation of ground-level $PM_{2.5}$ concentrations over Beijing using 3 km resolution MODIS AOD. Environ. Sci. Technol. 49, 12280–12288.

Xu, P., Chen, Y., Ye, X., 2013. Haze, air pollution, and health in China. Lancet 382, 2067.

You, W., Zang, Z., Zhang, L., Li, Y., Wang, W., 2016. Estimating national-scale ground-level $PM_{2.5}$ concentration in China using geographically weighted regression based on MODIS and MISR AOD. Environ. Sci. Pollut. Res. Int. 23, 8327–8338.

Yuan, Y., Liu, S., Castro, R., Pan, X., 2012. $PM_{2.5}$ monitoring and mitigation in the cities of China. Environ. Sci. Technol. 46, 3627–3628.

Zang, Z., Wang, W., You, W., Li, Y., Ye, F., Wang, C., 2017. Estimating ground-level $PM_{2.5}$ concentrations in Beijing, China using aerosol optical depth and parameters of the temperature inversion layer. Sci. Total Environ. 575, 1219–1227.

Zhang, Y.L., Cao, F., 2015. Fine particulate matter ($PM_{2.5}$) in China at a city level. Sci. Rep. 5, 14884.

Zhang, Q., He, K., Huo, H., 2012. Cleaning China's air. Nature 484, 161.

Zheng, Y., Zhang, Q., Liu, Y., Geng, G., He, K., 2016. Estimating ground-level $PM_{2.5}$ concentrations over three megalopolises in China using satellite-derived aerosol optical depth measurements. Atmos. Environ. 124, 232–242.

Zheng, C., Zhao, C., Zhu, Y., Wang, Y., Shi, X., Wu, X., et al., 2017. Analysis of influential factors for the relationship between $PM_{2.5}$ and AOD in Beijing. Atmos. Chem. Phys. 17, 13473–13489.

Zou, B., Pu, Q., Bilal, M., Weng, Q., Zhai, L., Nichol, J.E., 2016. High-resolution satellite mapping of fine particulates based on geographically weighted regression. IEEE Geosci. Remote Sens. Lett. 13, 495–499.